Molecular Structure Refinement of Polycrystalline Oriented Material by the Whole Fiber X-ray Diffraction Pattern Analysis[1]

Pio Iannelli

Department of Physics, University of Salerno, I-84100 Salerno, Italy

Received July 6, 1992; Revised Manuscript Received November 17, 1992

ABSTRACT: The whole fiber X-ray diffraction pattern analysis employing the theoretical profile function for fitting experimental spectra from a fiber sample of polycrystalline polymers is discussed. The method is based on the standard least squares fitting procedure. The molecular structure of polyisobutylene is investigated in order to refine both structural and morphological parameters, which are the averaged size and orientation angle of the crystallites around the fiber axis, and strain parameters.

Introduction

In 1967 Rietveld proposed a new method to analyze the neutron diffraction pattern from a powder sample of crystalline materials.[2,3] The comparison point-by-point of the observed neutron diffraction data with the calculated one by using the least squares fitting procedure avoids the peak-deconvolution process. To shape each diffraction peak, Rietveld employed a Gaussian function with the full width at half-maximum (FWHM) only depending on the diffraction angle 2θ according to Caglioti et al.[4] In 1977 the Rietveld method was applied to analyze the X-ray diffraction pattern from a powder sample of crystalline material.[5,6] As in the case of neutron diffraction, the FWHM of the diffraction peaks was parametrized as an empirical function of the 2θ angle by adjusting the parameters by means of the least squares fitting procedure. To improve the fitting, several functions were tested on an empirical basis, the most reliable of which are the Pearson VII distribution[7] and the pseudo-Voigt function.[8] Further improvements were achieved by several authors by introducing the *internal coordinates*,[7] i.e. bond lengths, bond angles, and torsion angles, instead of the atomic fractional coordinates, thus making it possible to reduce the number of parameters to be refined. Constraints[9] were also imposed, allowing, for instance, noncrystallographic symmetries within the asymmetric unit.

In the case of polymeric materials it is often possible to draw oriented samples (fibers), the diffraction patterns of which provide more information than those from unoriented samples because the Bragg spots may overlap only within layers. Following up the Rietveld idea, the *whole X-ray diffraction pattern* analysis was extended from the powder to the fiber case[10–13] to carry out molecular structure refinement. The most difficult step was how to represent the shape of each Bragg spot, a two-dimensional function being necessary, and in which *space* to perform the calculation. In fact one can carry out calculations either on the chosen *recording device*, defining an appropriate coordinate system,[14,15] or in the reciprocal space.[16] While the former case was already discussed,[10–12] showing that an empirical profile function may adequately reproduce the experimental pattern, in the latter case we showed only preliminary data:[17] the theoretical function depending on the morphological parameters was deduced and tested in fitting the whole diffraction pattern from a fiber sample of polyisobutylene (PIB), but no molecular structure refinement was performed. In this paper we will discuss the use of the above profile function for refining both the molecular structure and the morphological parameters of PIB.

Profile Function and Diffracted Intensity

Carrying out X-ray diffraction pattern fitting in the reciprocal space makes the molecular structure analysis independent of the diffraction geometry and it accounts for possible anisotropy of the crystallite size. According to a previous paper[17] we defined the intensity function (or profile function) T_k for shaping the kth reflection with Bragg indices hkl as the convolution between the *distribution function of the crystallite's orientation* $N(\alpha)$ about the fiber axis and the *convolute Laue function*, i.e. the cylindrically averaged Laue function $L(\xi,\eta,\zeta)$ by rotation about the fiber axis (η, ξ, and ζ are the fractional reciprocal coordinates). The most interesting feature of this profile function is that it depends only on the averaged crystallite size Δa, Δb, and Δc taken along the cell axes (respectively a, b, and c) and the averaged angle of crystallite orientation α_0 about the fiber axis.

The continuous diffraction intensity for fibrous samples of polycrystalline polymeric materials may be evaluated in the neighborhood of any Bragg reflection by placing

$$I_{k,i}(\Delta\rho_{k,i},\Delta\sigma_{k,i}) = I_k T_{k,i}(\Delta\rho_{k,i},\Delta\sigma_{k,i}) \qquad (1)$$

where I_k is the integrated intensity of the kth reflection, $\Delta\rho_{k,i} = \rho_i - \rho_k$, and $\Delta\sigma_{k,i} = \sigma_i - \sigma_k$. ρ_i, ρ_k and σ_i, σ_k are respectively the scattering vector $2(\sin\theta)/\lambda$ and the angle between ρ and the fiber axis of the sample. They are evaluated in the reciprocal space at the generic ith point and at the kth Bragg point.

As several reflections may contribute to a given point i, the total diffracted intensity is given by

$$I(\rho_i,\sigma_i) = S\sum_k I_k T_{k,i}(\Delta\rho_{k,i},\Delta\sigma_{k,i}) + B(\rho_i,\sigma_i) \qquad (2)$$

where the sum is extended over all reflections whose Bragg points are close to the current point. $B(\rho_i,\sigma_i)$, called the background, is the diffused diffraction intensity due to amorphous material and air[17] (see details in the Appendix), while S is a factor to scale the Bragg component of the diffraction with respect to the background. It is worth noting that eq 2 is independent of camera geometry because each experimental point can always be referred to the appropriate ρ_i,σ_i coordinates in the reciprocal space.

Anisotropic Thermal and Strain Parameters

In evaluating the diffracted intensity $I(\rho_i,\sigma_i)$ by eq 2, one should take into account the distortion of both the first and the second kind. The thermal vibration of atoms around their center, which affects the atomic scattering factors and consequently the integrated intensity I_k, is an example of distortion of the first kind. When a lattice

0024-9297/93/2226-2303$04.00/0

possesses distortion of the second kind, the cell parameters fluctuate more or less around their average. This affects both the integrated diffraction intensities and the profile function T_k, making it broader as the diffraction angle θ increases. The effect may be observed if two or more Bragg reflections belonging to the same *hkl* family but with different diffraction orders are detectable in the experimental pattern.

The two kinds of distortion may be either isotropic or anisotropic, in the sense that they may be independent of or dependent on the *direction* in the cell. With respect to the thermal disorder the isotropic model is the most applied in the case of polymeric material. When the anisotropic model is strictly necessary, one should take into account that the center of each atom is displaced along the direction of three axes orthogonal to each other. The displacement follows a Gaussian distribution named "ellipsoid of thermal vibration", and the thermal factor is just the Fourier transform of it, given by

$$f_{t_j} = \exp[-2\pi^2(\langle u_1^2\rangle x_1^2 + \langle u_2^2\rangle x_2^2 + \langle u_3^2\rangle x_3^2)] \quad (3)$$

x_1, x_2, x_3 and $\langle u_1^2\rangle$, $\langle u_2^2\rangle$, $\langle u_3^2\rangle$ are respectively the components of the scattering vector and the mean square displacement of the atom in the direction of the axes of the ellipsoid. If the axes of the ellipsoid do not coincide with those of the reference frame for the atomic coordinates, six parameters are necessary in order to evaluate f_t. This makes the anisotropic model generally not suitable for polymers for which few diffraction spots are usually observed. Moreover the diffraction is usually confined to the low angle region; thus the thermal parameters $\langle u_1^2\rangle$, $\langle u_2^2\rangle$, and $\langle u_3^2\rangle$ and the scale factor S are very often correlated[9] with respect to each other in the structure refinement. Thus to reduce the number of parameters to be refined, the directions of the three axes of the thermal ellipsoid may be fixed under the hypothesis that, due to the shape of the macromolecule, one of the axes coincides with the molecular chain, i.e. with the cell axis c. This hypothesis is a reliable one when no large molecular groups are side attached to the macromolecule backbone. The other two axes are perpendicular to the first one and their direction may be either fixed or refined according to the standard least squares procedure.

About the distortion of second kind, the diffracted intensity may be evaluated according to Hosemann's paracrystalline theory[18,19] by convolving the Laue function $L(\rho)$, depending on the crystallite size, with the paracrystalline factor $Z(\rho)$, depending on the lattice distortion:

$$C(\rho) = Z(\rho) * L(\rho) \quad (4)$$

If one supposes that the cell parameter distribution is Gaussian (Guinnier's approximation) and independent of *hkl* indices, the $Z(\rho)$ factor is well approximated by the product of three one-dimensional Gaussian functions[20,21]

$$Z(\rho) = Z(\xi)Z(\eta)Z(\zeta) \quad (5)$$

where, for example,

$$Z(\xi) = \frac{1}{\pi^2 h^2 g_a^2} \exp\left[-\left(\frac{\xi}{\pi^{3/2} h^2 g_a^2}\right)^2\right] \quad (6)$$

The fractional coordinates ξ, η, and ζ are placed at zero at the Bragg points, and they are related to the reciprocal coordinates ξ^*, η^*, and ζ^* by

$$\xi^* = (\xi + h)a^* \qquad \eta^* = (\eta + k)b^* \qquad \zeta^* = (\zeta + l)c^*$$

where a^*, b^*, and c^* are the reciprocal cell parameters. g_a is the strain parameter which is the measure of the distortion of the second kind. It is defined as the ratio $\sigma_a/\langle a\rangle$ between the standard deviation σ_a of the Gaussian distribution of cell parameter a and its average $\langle a\rangle$. An analogous expression can be written for $Z(\eta)$ and $Z(\zeta)$. It should be kept in mind that eq 6 can be applied only for small values of g parameters, when the Gaussian approximitation is applicable.

In order to account for the paracrystalline effect in the profile fitting we may lightly modify the profile function T_k according to the procedure followed in ref 17 where the Laue function was approximated by the product of three Gaussians

$$L(\rho) = L(\xi)L(\eta)L(\zeta) \quad (7)$$

where, for example,

$$L(\xi) = \Delta a a^* \exp[-\pi(\Delta a a^* \xi)^2] \quad (8)$$

By application of eqs 5 and 7 to eq 4, $C(\rho)$ becomes the product of three convolutions

$$C(\rho) = C(\xi)C(\eta)C(\zeta) = L(\xi) * Z(\xi)L(\eta) * Z(\eta)L(\zeta) * Z(\zeta) \quad (9)$$

Due to the well-known property of the Gaussian function, each term C in eq 9 is Gaussian with the standard deviation

$$\sigma_C^2 = \sigma_L^2 + \sigma_Z^2 \quad (10)$$

however, according to eqs 6 and 8

$$\sigma_{C_\xi}^2 = \frac{1}{\pi a^{*2} \Delta a^2} + \pi^3 h^4 g_a^4 = \frac{1}{\pi}\left(\frac{1}{a^{*2}\Delta a^2} + \pi^4 h^4 g_a^4\right) \quad (11)$$

Analogous expression can be written for σ_{C_η} and σ_{C_ζ}.

By using $C(\rho)$ instead of $L(\rho)$ in deducing the profile function T_k as made in ref 17, one obtains a new analytical expression for T_k (see Appendix for details) able to account for lattice distortion of the second kind.

Extention of the Rietveld Method to the Oriented System

The following three hypotheses were made in deducing the T_k profile function in ref 17: (i) the crystallites are supposed to grow along the cell edges, (ii) the instrumental function, i.e. the instrumental contribution to the data broadening, is negligible, and (iii) all crystallites have the same size. If the hypothesis at point i is not right, it is always possible to define the appropriate auxiliary *cell* corresponding to the true crystal shape and to refine the edge dimensions of such a *cell*. The assumption at point ii, which is exact only if an excellent collimated and monochromatized X-ray beam is used, may be in most cases a good approximation for polymers because of the small size of the crystallites for this kind of material. Point iii needs more attention because the hypothesis that all the crystallites have the same size is not reliable and seems to be an ad hoc one. Anyway a narrow distribution of crystallite size should not affect substantially the profile function T_k and the morphological parameters Δa, Δb, and Δc should save their meaning at least as averaged parameters. On the other hand a broad distribution of crystallite size does affect T_k and Δa, Δb, and Δc should be treated as *fitting* parameters only.

By keeping in mind the previous considerations, T_k can be employed for carrying out molecular structure refinement by comparing the observed diffracted intensity $I_{obsd,i}$ with the calculated one $I_{calcd,i}$. This may be done by employing the standard least squares procedure which we already discussed in refs 10–12. The diffracted pattern is evaluated by eq 2 as a function of both nonstructural parameters, affecting T_k and B, and structural ones,

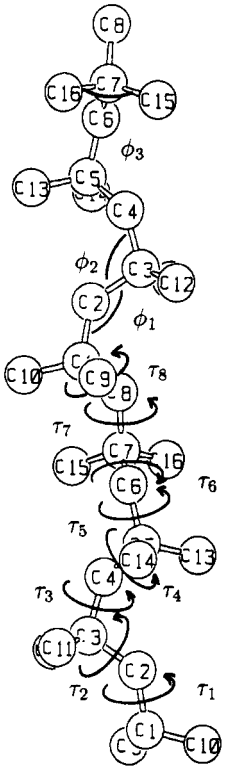

Figure 1. Structural parameters for building the molecular chain of polyisobutylene.

affecting the integrated intensities $I_k = mPF_k^2$ (m, P, and F_k are respectively the multiplicity, polarization factor, and structural factor). The Lorentz factor is already accounted for by the profile function T_k.[17] An iterative refinement is carried out in order to obtain the best parameters which minimize the quantity

$$\sum_i w_i[I_{\text{obsd},i} - I_{\text{calcd},i}]^2 \qquad (12)$$

where w_i is the statistical weight of the observations and $I_{\text{obsd},i}$ and $I_{\text{calcd},i}$ are respectively the observed and calculated diffracted intensity. If the "multiple-film" technique is employed,[10,12] $I_{\text{calcd},i}$ is given by

$$I_{\text{calcd},i} = S_j I(\rho_i, \sigma_i) \qquad (13)$$

where S_j are suitable factors to scale the diffracted intensity. As many S_j factors are taken as there are films recorded at different exposure times.

Thus, as preliminary test, the molecular structure of polyisobutylene,[22] space group $P2_12_12_1$, was refined in order to compare the results with those already reported by us for the same material but fitting the experimental pattern by means of an empirical profile function.[11,12] The experimental data are the same used in the previous paper as obtained by digitizing and merging four films taken at different exposure times in the approximative ratio 1:1.5:9:12. Only the structure model with local C_{2v} symmetry for each quaternary carbon atom, among those discussed in ref 12, was refined.

The strategy adopted in carrying out the structure refinement was (i) all morphological parameters, scale factors, and cell parameters were refined by keeping fixed the internal coordinates defined in Figure 1 at the values given in Table I, column B, and (ii) all the parameters, including the internal coordinates, were refined together. Refinements were stopped when parameter fluctuations were less than the standard deviations. The agreement between observed and calculated data is better than the previous one (see Figures 2 and 3) but, in spite of this, the structural parameters are almost the same (see Table I). It is worth noting that the averaged crystallite size is very close to that obtained in ref 17 where only pattern fitting was performed without any structure analysis. The value obtained for the parameter g_a suggests that the cell lattice is lightly distorted in the direction of axis a.

The atomic coordinates of the refined structure are listed in Table II.

Table I
List of the Parameters As Obtained after the Molecular Structure Refinement of Polyisobutylene According to This Paper (A), to Reference 12 (B), and to Reference 17 (C)[a]

	A	B	C
a	6.90(1)	6.88	6.88
b	11.92(1)	11.91	11.91
c	18.60(1)	18.60	18.60
Δa (Å)	117(1)		127(1)
Δb (Å)	116(1)		108(1)
Δc (Å)	74.4(4)		73.2(2)
α (deg)	5.52(1)		5.60(1)
g_a	1.92(2)		
g_b	0.01(2)		
g_c	0.10(2)		
ϕ_1	132.1(1)	129.2(2)	
ϕ_2	108.8(1)	109.9(1)	
ϕ_3	110.6(1)	110.7(1)	
τ_1	47.9(3)	48.4(2)	
τ_2	167.6(2)	167.7(2)	
τ_3	53.6(1)	60.0(2)	
τ_4	161.0(2)	156.4(2)	
τ_5	51.7(1)	53.7(2)	
τ_6	169.3(2)	166.7(2)	
τ_7	60.6(1)	54.9(2)	
τ_8	166.6(2)	163.6(3)	
z_0 (Å)	0.893(1)	0.873(2)	
Φ_0 (deg)	−29.3(1)	−36.1(2)	
$\langle u^2\rangle_{\text{iso}}$ (Å^2)	0.0237(2)	0.0156	
S	7.48(4)		
S_1	0.0785(5)		
S_2	0.174(1)		
S_3	1.432(7)		
S_4	2.09(1)		
ϵ_1	−71.7(1)		
ϵ_2	573.6(5)		
ϵ_3	−725(1)		
g_1	15.7(1)		
g_2	0.1020(3)		
g_3	0.1138(7)		
$R_{p,1}$	0.095	0.059	0.077
$R'_{p,1}$	0.346		
$R_{p,2}$	0.060	0.106	0.088
$R'_{p,2}$	0.298		
$R_{p,3}$	0.041	0.056	0.037
$R'_{p,3}$	0.397		
$R_{p,4}$	0.023	0.059	0.020
$R'_{p,4}$	0.490		

[a] Standard errors are given in parentheses. C–C and C–H bond lengths were fixed respectively to 1.54 and 1.08 Å. z_0 is the z coordinate of carbon atom C_1, while Φ_0 is the angle of overall rotation of the molecule around its own chain axis. Φ_0 is placed at zero when the chain axis and the carbon atom C_1 lay in a plane parallel to the $x-y$ plane. Hydrogen atoms were included in the calculation by evaluating atomic coordinates according to sp^3 geometry. The four discrepancy R_p and R'_p indices are referred to the four films with different exposure times. In evaluating R'_p, we took into account only the experimental points with a Bragg contribution to the intensity higher than the experimental error (about 3% of the observed intensity). The nonstructural parameters ϵ_i and g_i are defined in the Appendix. The strain parameters g_a, g_b, and g_c are given in percent.

Some Considerations about the Discrepancy Index

The major feature of a good discrepancy index is to compare the *goodness* of several structural models. Depending on the fitting procedure, ad hoc discrepancy

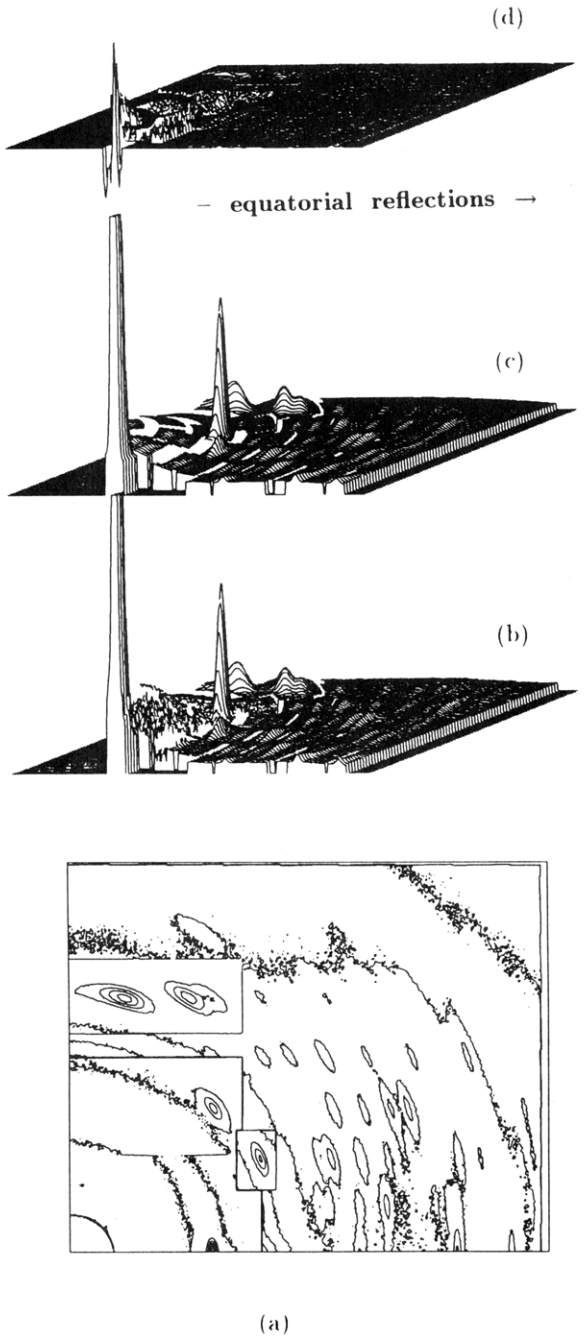

Figure 2. (a) Digitized image of the observed diffraction pattern of a stretched sample of polyisobutylene (Ni-filtered Cu Kα radiation) used for carrying out structure refinement. The observed (b) and the calculated (c) diffraction spectra after refinement, and the relative difference (d), are shown in the same scale. The intensity is reduced by one-third to show the weaker part of the pattern.

indexes may be needed. The most used is

$$R_p = \frac{\sum_i |I_{obsd,i} - I_{calcd,i}|}{\sum_i I_{obsd,i}} \quad (14)$$

For those techniques which use the integrated intensities as experimental data, like the linked atom least squares (LALS) procedure,[23] R_p may depend on the way one subtracts the diffuse contribution from each diffraction spot, especially in the case where very broad reflections are observed. When the whole pattern method is em-

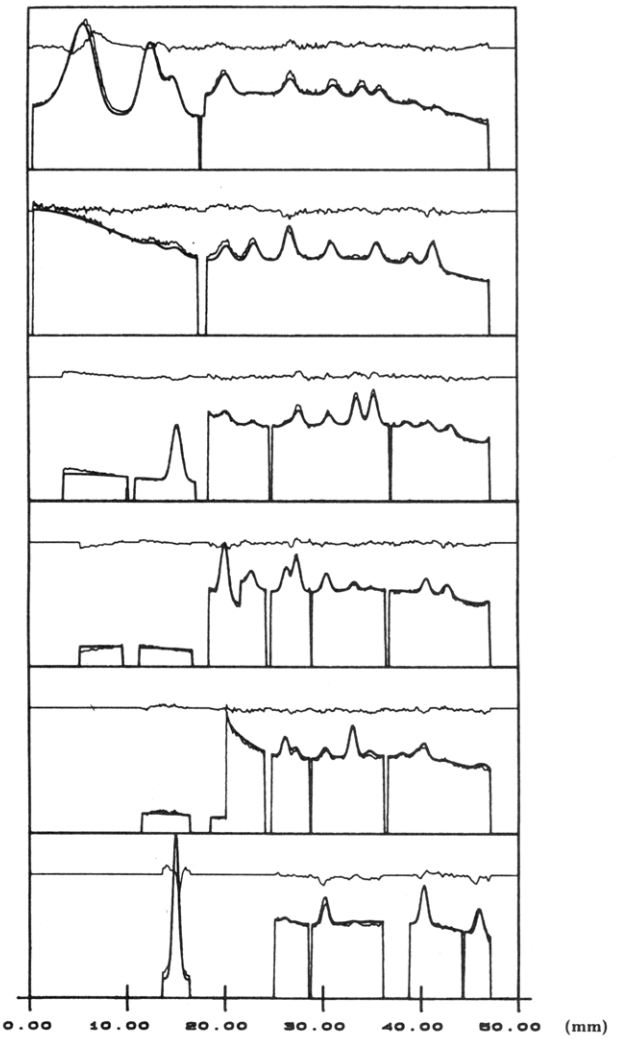

Figure 3. Observed (thin line) and calculated (thick line) diffraction intensities compared along the layer lines. The Bragg index l goes from 0 (bottom) to 5 (top). The difference between the observed and the calculated intensities is also shown by a continuous thin line lightly shifted.

Table II
List of the Atomic Coordinates As Obtained after Molecular Structure Refinement of Polyisobutylene

C_1	0.373(1)	0.040(3)	0.048(1)
C_2	0.341(1)	0.022(1)	0.129(1)
C_3	0.156(1)	0.017(1)	0.175(1)
C_4	0.214(1)	0.022(1)	0.255(1)
C_5	0.355(1)	−0.049(2)	0.300(2)
C_6	0.305(1)	−0.033(1)	0.381(2)
C_7	0.278(2)	0.072(3)	0.427(1)
C_8	0.268(2)	0.037(1)	0.507(2)
C_9	0.312(2)	0.159(5)	0.026(1)
C_{10}	0.590(3)	0.031(2)	0.029(2)
C_{11}	0.040(3)	−0.090(3)	0.159(3)
C_{12}	0.020(2)	0.116(4)	0.156(3)
C_{13}	0.566(2)	−0.014(2)	0.286(3)
C_{14}	0.341(3)	−0.173(4)	0.279(3)
C_{15}	0.092(3)	0.135(4)	0.405(3)
C_{16}	0.445(3)	0.156(4)	0.415(3)

ployed, R_p is affected by the relative position of experimental and calculated Bragg spots, thus resulting in R_p as a more severe index for this technique. Moreover the absolute value of the diffused intensity B_i in eq 2 may strongly affect R_p,[24] for instance, in the two following cases: (i) diffused intensity much higher than the diffracted one and (ii) diffracted intensity comparable to the diffused one. In the former case $I_{obsd,i} \sim B_i$ and R_p becomes

$$R_p = \frac{\sum_i |I_{obsd,i} - I_{calcd,i}|}{\sum_i I_{obsd,i}} \sim \frac{\sum_i |I_{obsd,i} - I_{calcd,i}|}{\sum_i B_i} \quad (15)$$

Following that high value of B_i makes R_p small and quite independent of the goodness of molecular structure refinement. In the latter case R_p may be influenced by points far from Bragg spots which are not correlated to the molecular structure. In both cases R_p may not be reliable for evaluating discrepancy. To make R_p meaningful, one should take into account only experimental points close to the Bragg spots, removing the problem raised at point ii. About point i the problem is only partially solved because the diffused intensity is always higher than the diffracted one even for those points close to the Bragg spots. Thus it may be appropriate to subtract the background from the observed intensity, evaluating the discrepancy index[24] as

$$R'_p = \frac{\sum_i |I_{obsd,i} - I_{calcd,i}|}{\sum_i |I_{obsd,i} - B_i|} \quad (16)$$

where the summation should be carried out including only those points where the Bragg contribution to the intensity is significant. R'_p, which was recently introduced in the Rietveld analysis,[24] is a more severe discrepancy index than R_p. In the case of whole fiber pattern analysis here discussed, R'_p reaches very high values, being strongly dependent on the position of the Bragg spots due to the two-dimensional feature of the pattern. For instance, in the case of the molecular structure refinement of PIB, R'_p ranges between 0.30 and 0.50 (see Table I) in spite of the good consistency between calculated and observed patterns (see Figures 2 and 3). This suggests that even R'_p is not a reliable index and that particular care should be taken to use both R_p and R'_p for structure refinement purposes. Thus graphical comparison between calculated and observed data seems always opportune to judge the goodness of molecular structure refinement.

Conclusion

We have shown that the whole fiber pattern analysis for refining the molecular structure and the morphological parameters together by employing the profile function discussed in this paper and in the previous one[17] is a reliable method. The profile function T_k has been modified in this paper in order to include strain parameters according to the paracrystalline theory.

To improve the method, the following points may need further attention in the future, concerning both experimental techniques and data processing.

(i) The instrumental broadening, especially for large crystallite size, should be reduced by improving both beam collimation and the monochromaticity of radiation. The use of synchrotron radiation could be very useful.

(ii) The photographic recording suffers from errors which becomes large if the intensity range is wide, making the multiple-film technique necessary. For this purpose area detectors may be employed for avoiding scaling errors.

(iii) The background contribution (incoherent scattering, diffraction by amorphous material, etc.) should be evaluated, if possible, by using a less arbitrary approach. Semiempirical methods,[25] as applied to an unoriented polycrystalline sample, could be considered when the diffraction spectra from the pure amorphous component of the fiber sample is available. Indeed, several experimental problems may arise, because the amorphous component is very often partially oriented too. To obtain pure oriented amorphous sample is not easy, especially if crystallinity is induced, for instance, by the drawing process.

Acknowledgment. Financial support by the Ministero dell'Universitá e della Ricerca Scientifica e Tecnologica and by the Comitato Nazionale delle Ricerche is acknowledged.

Appendix

Background Parameters. The $B(\rho_i,\sigma_i)$ diffused intensity in eq 2 is assumed to be the sum of three contributions according to ref 17, placing $\xi_i = \rho_i \sin(\sigma_i)$ and $\zeta_i = \rho_i \cos(\sigma_i)$:

$$B(\rho_i,\sigma_i) = B^{(u)}(\xi_i,\zeta_i) + B^{(i)}(\rho_i) + B^{(a)}(\xi_i,\zeta_i) \quad (17.1)$$

where

$$B^{(u)}(\xi_i,\zeta_i) = \epsilon_1 + \epsilon_2\xi_i + \epsilon_3\xi_i^2 + \epsilon_4\zeta_i + \epsilon_5\zeta_i^2 \quad (17.2)$$

however, for isotropic contribution

$$B^{(u)}(\rho_i) = \epsilon_1 + \epsilon_2\rho_i + \epsilon_3\rho_i^2 \quad (17.3)$$

and

$$B^{(i)}(\rho_i) = \sum_m \frac{g_{1_m}}{g_{2_m}} \exp\left[-\left(\frac{\rho_i - g_{3_m}}{g_{2_m}}\right)^2\right] \quad (17.4)$$

$$B^{(a)}(\xi_i,\zeta_i) = \sum_m \frac{f_{1_m}}{f_{2_m} f_{3_m}} \exp\left[-\left(\frac{\xi_i - f_{4_m}}{f_{2_m}}\right)^2\right] \times \exp\left[-\left(\frac{\zeta_i - f_{5_m}}{f_{3_m}}\right)^2\right] \quad (17.5)$$

$B^{(u)}$ is the incoherent scattering which is a decreasing function of ρ_i (17.3) (isotropic case) or of its components ξ_i and ζ_f (17.2) (anisotropic case); $B^{(i)}$ is the isotropic scattering of the unoriented and amorphous competent of the sample, and it consists of the sum of several haloes with Gaussian intensity distributions; $B^{(a)}$ is the anisotropic scattering of the oriented and amorphous component of the sample, and it consists of the sum of several *streaks* orthogonal to the fiber axis. In the molecular structure analysis of polyisobutylene discussed in this paper only the two terms $B^{(u)}$ (17.3) and $B^{(i)}$ (17.4) were evaluated.

Profile Function and Strain Parameters. The matrix **U** in eq 12 of ref 17

$$\mathbf{U} = \tilde{\mathbf{M}}\cdot\mathbf{D}\cdot\mathbf{M} \quad (18)$$

has to be modified in order to include strain parameters in the analytical expression of profile function T_k. **U** allows one to approximate the Laue function (eq 11 in ref 17) by

$$L(x,y,z) = N_t^2 \exp[-(x,y,z)\mathbf{U}\{x,y,z\}] \quad (19)$$

where N_t is the product of the numbers of cell repetition along the direction of each lattice axis. **M** in eq 19 is the matrix which transforms the orthogonal reciprocal coordinates x, y, and z (Å^{-1} units) into the fractional reciprocal coordinates ξ, η, and ζ. The diagonal matrix **D** is the only matrix which has to be modified according to the new variances given in eq 11. Thus the new diagonal terms of matrix **D** are $1/\sigma_{C_\xi}{}^2 a^{*2}$, $1/\sigma_{C_\eta}{}^3 b^{*2}$, and $1/\sigma_{C_\zeta}{}^2 c^{*2}$.

References and Notes

(1) This work was presented in part at the XIV Congress of IUCr in Bordeaux, July, 1990: Iannelli, P.; Immirzi, A. *Acta Crystallogr.* **1990**, *A46*, C-54.
(2) Rietveld, H. M. *Acta Crystallogr.* **1967**, *22*, 151.
(3) Rietveld, H. M. *J. Appl. Crystallogr.* **1969**, *2*, 65.
(4) Caglioti, G.; Paoletti, A.; Ricci, F. P. *Nucl. Instrum.* **1958**, *3*, 223.
(5) Malmros, G.; Thomas, J. O. *J. Appl. Crystallogr.* **1977**, *10*, 7.
(6) Young, R. A.; Mackie, P. E.; Von Dreele, R. B. *J. Appl. Crystallogr.* **1977**, *10*, 262.
(7) Young, R. A.; Lundberg, J. L.; Immirzi, A. In *Fiber Diffraction Methods*; French & Gardner, Eds.; ACS Symposium Series 141; American Chemical Society: Washington, DC, 1980; pp 69–91.
(8) Toraya, H. *Powder Diffr.* **1989**, *4*, 130.
(9) Tadokoro, H. *Structure of Crystalline Polymer*; J. Wiley & Sons: New York, 1979; Chapter 8, p 139 (see also references therein).
(10) Immirzi, A.; Iannelli, P. *Macromolecules* **1988**, *21*, 768.
(11) Iannelli, P.; Immirzi, A. *Macromolecules* **1989**, *22*, 196.
(12) Iannelli, P.; Immirzi, A. *Macromolecules* **1989**, *22*, 200.
(13) Busing, W. R. *Macromolecules* **1990**, *23*, 4608.
(14) Makowski, L. In *Fiber Diffraction Methods*; French & Gardner, Eds.; ACS Symposium Series 141; American Chemical Society: Washington, DC, 1980; p 139.
(15) Millane, R.; Arnott, S. *J. Macromol. Sci., Phys.* **1985–1986**, *B24* (1–4), 193.
(16) Fraser, R. D. B.; MacRae, T. P.; Miller, A.; Rowlands, R. J. *J. Appl. Crystallogr.* **1976**, *9*, 81.
(17) Iannelli, P.; Immirzi, A. *Macromolecules* **1990**, *23*, 2375.
(18) Hosemann, R.; Wilke, W. *Makromol. Chem.* **1968**, *118*, 230.
(19) Buchanan, D. R.; Miller, R. L. *J. Appl. Phys.* **1966**, *37*, 4003.
(20) Vainshtein, B. K. *Diffusion of X-ray by chain molecules*; Elsevier: New York, 1966; Chapter 5, pp 216–240 (see also references therein).
(21) Tadokoro, H. *Structure of Crystalline Polymer*; J. Wiley & Sons: New York, 1979; Chapter 4, p 146–150 (see also references therein).
(22) Tanaka, T.; Chatani, Y.; Tadokoro, H. *J. Polym. Sci., Polym. Phys. Ed.* **1974**, *12*, 112.
(23) Boon, J.; Magre, E. P. *Makromol. Chem.* **1969**, *126*, 130.
(24) Hill, R. J.; Fischer, R. X. *J. Appl. Crystallogr.* **1990**, *23*, 462.
(25) Polizzi, S.; Fagherazzi, G.; Benedetti, A.; Battagliarin, M. *J. Appl. Crystallogr.* **1990**, *23*, 359 and references therein.